METHODS, TOOLS, AND TECHNOLOGIES

Effects of camera-trap placement and number on detection of members of a mammalian assemblage

TIM R. HOFMEESTER [iD],[1],† NERI H. THORSEN,[2] JORIS P. G. M. CROMSIGT [iD],[1,3,4] JONAS KINDBERG [iD],[1,5] HENRIK ANDRéN [iD],[6] JOHN D. C. LINNELL [iD],[5,7] AND JOHN ODDEN [iD][2]

[1]Department of Wildlife, Fish, and Environmental Studies, Swedish University of Agricultural Sciences, Umeå SE-90183 Sweden
[2]Norwegian Institute for Nature Research, Sognsveien 68, Oslo NO-0855 Norway
[3]Department of Zoology, Centre for African Conservation Ecology, Nelson Mandela University, Port Elizabeth 6031 South Africa
[4]Copernicus Institute of Sustainable Development, Environmental Sciences, Utrecht University, Utrecht 3548 The Netherlands
[5]Norwegian Institute for Nature Research, PO Box 5685 Torgard, Trondheim NO-7485 Norway
[6]Department of Ecology, Swedish University of Agricultural Sciences, Grimsö Wildlife Research Station, Riddarhyttan
SE-73993 Sweden
[7]Department of Forestry and Wildlife Management, Inland Norway University of Applied Sciences,
Koppang NO-2480 Norway

Abstract. A central goal in camera-trapping (CT) studies is to maximize detection probability and precision of occupancy estimates while minimizing the number of CTs to reduce equipment and labor costs. Few studies, however, have examined the effect of CT number on detection probability. Moreover, historically, most studies focused on a specific species and the design could be tailored toward maximizing detection of this target species. Increasingly, however, such studies use data for all captured, non-target, species (by-catch data) for animal community-level analyses. It remains unclear if, and how, the targeting of CTs toward one species affects the detection of non-target species. We paired CTs from a permanent camera-trapping grid (with 38 CTs) targeted at monitoring Eurasian lynx (*Lynx lynx*) in Innlandet County, Norway, with additional randomly placed CTs at two spatial scales (38 CTs within the same habitat patch and 38 CTs within the same 50-km^2 grid cell as the lynx-targeted CTs) for three months. We combined multi-scale occupancy models that enable the separation of large-scale occupancy, CT-scale site use, and detection probability with single-scale occupancy models. This allowed us to study the effects of targeted placement and CT number on the detection probability of the target species (lynx) and seven non-target mammal species (four carnivores, three herbivores, and one rodent). We found that all species, except moose (*Alces alces*), had the highest detection probability at lynx-targeted CTs. Moose had equal detection probabilities at all three placement types. Adding extra CTs generally increased detection probabilities. Consequently, for all species, combining a lynx-targeted CT with one or more randomly placed CTs, increased the accuracy and precision of occupancy estimates for 50-km^2 grid cells compared to single CT estimates. The placement of single CTs underestimated grid-cell occupancy compared to known minimum occupancy and were similar to site-use probability estimates of multi-scale models. It is, however, uncertain to which spatial extent these site-use probabilities refer. We therefore recommend the use of multiple (targeted) CTs to estimate occupancy in large grid cells and to interpret occupancy estimates from single CTs as site use of an, as of yet undefined, area surrounding the CT.

† **E-mail:** tim.hofmeester@slu.se

INTRODUCTION

Remote cameras activated by a passive infrared (PIR) sensor, known as camera traps or trail cameras (from here on referred to as CTs), are increasingly used to study wildlife (Burton et al. 2015). Camera-trap studies are often targeted at large carnivores and tailor their design to increase the detection probability for these species, as research and conservation funding is most often directed at the larger, more endangered, charismatic and/or more conflict-prone, species (Linnell et al. 2000). As the PIR sensor is relatively unselective in which species it detects (but see, e.g., Hofmeester et al. 2017 for the effect of body size on detectability), CT surveys targeted at large carnivores can potentially be used to look at non-target species or even whole mammal communities (Tobler et al. 2008, Rich et al. 2016, Mazzamuto et al. 2019). However, in these scenarios, biases in detection of non-target species, for example, due to differences in movement ecology, habitat preferences, or inter-species interactions, are crucial to know, but are poorly studied (but see, e.g., Harmsen et al. 2010).

Camera-trap data are often analyzed using hierarchical models, such as occupancy models or spatially explicit capture–recapture models, that separate the detection process from the ecological state of interest to correct for imperfect detection (Burton et al. 2015, Kéry and Royle 2016, Sollmann 2018). Occupancy models, and derived models such as the Royle-Nichols model, estimate detection probability based on the detection history—a record of detections and non-detections over several surveys or periods—of a species at each site (MacKenzie et al. 2002, 2006, Royle and Nichols 2003). These detection probabilities are then used to estimate the probability of occurrence at sites where the species was not detected. Low detection probabilities can result in biased estimates of occupancy (MacKenzie et al. 2002), while the precision of the occupancy estimate is determined by the combination of detection probability and the number of surveys (Mackenzie and Royle 2005). Optimizing

CT placement to increase detection probability is thus important for obtaining unbiased and precise estimates of occupancy, specifically when studying rare species such as large carnivores.

Specific targeting of CTs to record large carnivores can potentially affect the inference which can be drawn for other species at different (spatial) scales (Hofmeester et al. 2019). At a landscape scale, CTs might be biased in the habitat type in which they are placed. Most studies aimed at detecting big cats place CTs specifically in parts of the landscape where signs indicate the presence of the species (Karanth and Nichols 1998, Jackson et al. 2006, Gimenez et al. 2019) thereby selecting for preferred habitat types of the target species. This landscape scale bias might influence the presence of non-target species in the direct surroundings of the CT, which might influence the detection probability, and consequently inference on state parameters, such as presence or density, of these species. At the same time, CTs might be biased toward certain microsites. For example, studies aimed at large carnivores often target their CTs by placing them on roads or trails (Tobler et al. 2008, Rich et al. 2016). This has been shown to affect the detection probability of different species, potentially influencing the inference on state parameters (Kolowski and Forrester 2017, Iannarilli et al., *unpublished manuscript*, Fonteyn et al., 2021).

The effects of the above-mentioned biases on inference are also related to how the state parameter derived from CT data is interpreted. Camera traps are often used to estimate the occupancy probability of mobile species at specific locations (point samples) in a continuous habitat, where occupancy is interpreted as site use (or 3rd order habitat selection sensu Johnson 1980) if single home ranges overlap with multiple CTs (Mackenzie and Royle 2005, Efford and Dawson 2012, Steenweg et al. 2018). However, there are also studies interpreting occupancy probabilities at CT sites as the occurrence of a species in some part of the landscape (or 2nd order habitat selection sensu

Johnson 1980), often represented as grid cells the size of a species home range in both theoretical (Efford and Dawson 2012, Steenweg et al. 2018), and empirical studies (e.g., Linden et al. 2017, Davis et al. 2018). A single CT in a larger grid cell can only detect the species if two conditions are met: (1) the species is using the specific habitat patch where the CT is located if it is present in the grid cell, and (2) the CT is placed in a microsite where the animal passes the CT when the species uses the habitat patch (Efford and Dawson 2012, Hofmeester et al. 2019). In other words, the CT needs to be located in a habitat type and microsite that are used by the target species if it occurs in the grid cell or it will never be detected. As long as some CTs are placed in used sites, resulting in non-zero detection probabilities, occupancy modeling can be used to model differences in detection probability due to microsite and habitat covariates. However, it is unclear if such a single CT approach to estimate occupancy in larger grid cells would result in a sufficiently high detection probability for non-target species to get precise occupancy estimates, as it is more likely that one or both conditions are not met for these species.

An additional approach to increase detection probability that is not as species-specific as targeted placement is the use of multiple CTs to estimate occupancy at a single site or grid cell. Several recent studies have shown that using multiple CTs to sample a site results in increased detection probability with consequently increased precision of occupancy estimates (Pease et al. 2016, Evans et al. 2019, Wong et al. 2019). This is likely because the use of multiple CTs increases the likelihood that at least one of them is situated in a site that is used by the species. However, all of these studies focused on multiple CTs within a short distance of each other, whereas spreading out several CTs over a grid cell would theoretically result in a better sampling of that grid cell. Furthermore, these studies did not directly compare the effects of targeted placement, the number of CTs, and their combination, on detection probabilities. Therefore, studies are needed that test the effect of targeting a CT on specific microsites, as well as the number of CTs used on occupancy metrics of

targeted and non-targeted species at different spatial scales and sampling units.

In this study, we quantified the influence of CT placement targeted at monitoring Eurasian lynx (*Lynx lynx*) as well as the number of CTs on detection probabilities in an assemblage of non-target mammal species at different spatial scales in a boreal forest landscape in southeastern Norway. We paired targeted CTs (38 CTs placed in sites known or expected to be frequented by lynx) with random CTs at two spatial scales (38 CTs within the same habitat patch and 38 CTs further away but within the same 50 km²-grid cell). We used Bayesian single- and multi-scale occupancy models to disentangle factors influencing detection, site use, and occupancy probability. We additionally tested for the effect of the targeting, number, and spacing of CTs on detection probability estimates at the grid-cell level, as well as accuracy and precision of occupancy probability estimates, by splitting our data into several subsets to mimic different study designs. Lastly, we used the different subsets to investigate potential bias in identifying the effects of covariates on occupancy under varies sampling designs.

MATERIALS AND METHODS

Camera-trap survey

Our study was conducted in Innlandet County (formerly Hedmark County), Norway (~9700 km², 61° N, 12° E) situated in the boreal zone (Fig. 1). Extensive boreal forest tracts and relatively low human population densities characterize the area. Moreover, it hosts breeding populations of four large carnivore species—brown bear (*Ursus arctos*), wolf (*Canis lupus*), Eurasian lynx and wolverine (*Gulo gulo*)—and several other larger mammal species such as moose (*Alces alces*), red deer (*Cervus elaphus*), roe deer (*Capreolus capreolus*), badger (*Meles meles*), red fox (*Vulpes vulpes*), pine marten (*Martes martes*), and mountain hare (*Lepus timidus*). The topography consists of several parallel river valleys running from northwest to southeast at about 200–300 m above sea level, separated by hills ranging from 600 to 800 m a.s.l. Innlandet is one of the counties in which the SCANDCAM project has volunteer-run CTs (HC500, PC900 & HP2X, Reconyx, Holmen, Wisconsin, USA) to

$z_i \sim Bernoulli(\psi_i)$
$a_{i,j}|z_i \sim Bernoulli(z_i \times \theta_{i,j})$
$y_{i,j,k}|a_{i,j} \sim Bernoulli(a_{i,j} \times p_{i,j,k})$

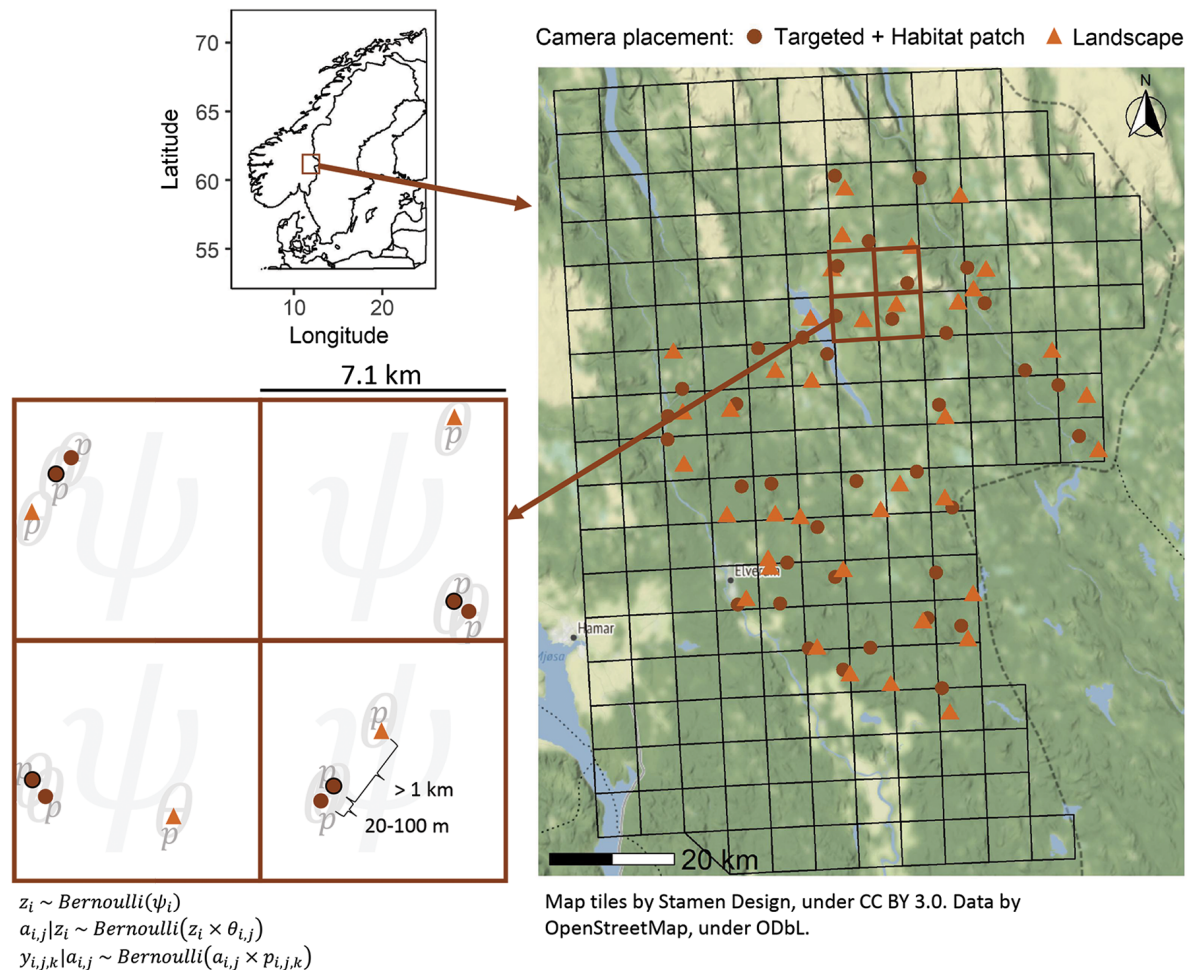Map tiles by Stamen Design, under CC BY 3.0. Data by OpenStreetMap, under ODbL.

Fig. 1. Study design and location. Upper left panel shows the location of the study area on the border of Norway and Sweden. Right panel shows the camera trap (CT) sites for targeted and random CTs at habitat-patch scale (circles; due to scale the difference of <100 m is not visible) and random CTs at landscape scale (triangles) distributed over the 50-km^2 grid. Background of right panel shows the hills to the north and east of the study area and the river and agricultural fields in the west. The lower left shows a schematic representation of the study design and the different parameters as included in the multi-scale occupancy model, where the occupancy probability (ψ) estimates the probability that the species occurs in a single 50-km^2 grid cell, the site-use probability (θ) estimates the probability of the species using the habitat directly surrounding each CT given that it occupies the grid cell, and the detection probability (p) estimating the likelihood of a species being detected by the CT given it is using the direct surroundings of the CT. Furthermore, it shows the distance restrictions used when generating the random CT sites: a distance of 20–100 m from the targeted CT for the habitat-patch CT and a distance of >1 km for the random landscape CT.

monitor lynx family groups (see viltkamera.nina.no for sites and data). Local volunteers selected the site of the CTs placing one lynx-targeted CT in each 50-km^2 grid cell that covers the area (Fig. 1). Volunteers were asked to place the CT at a site where they had seen tracks of lynx while snow tracking for lynx monitoring. If they never found lynx tracks in the grid cell, they were asked to locate the CT on a type of microsite that is often used by lynx to travel, such as a forest road, along the base of a cliff or on a wildlife trail. Camera traps were operated year-round

since the winter of 2013/2014, with volunteers switching SD cards and batteries every couple of months as needed.

For this study, we selected 38 of the lynx-targeted CTs that were active in the area. We paired each targeted CT with two random CTs (HC500, Reconyx, Holmen, Wisconsin, USA) at two spatial scales. The habitat-patch CT was placed in a randomly generated location within 20–100 m from the lynx-targeted CT within forest as based on the forest layer of the Norwegian National Land-cover map (Kartverket, Hønefoss, Norway). We did this to enable differentiation at the microsite scale as the CT was placed in the same habitat patch as the targeted CT, but in a different microsite. Similarly, we placed the landscape CT in a randomly generated location within forest in the same 50-km^2 grid cell. We did this to make sure it was deployed in the same part of the landscape and in the same habitat type, but in a different habitat patch (>1 km from the targeted CT) to disentangle effects at the habitat-patch scale as well as enable estimation of occupancy probability for each grid cell based on multiple CTs sampling different parts of the landscape (Fig. 1). Note that all CTs were placed in forest habitat.

We swapped SD cards and batteries for lynx-targeted CTs while deploying the random CTs to ensure the same battery type (Energizer Ultimate Lithium, Energizer Brands, St. Louis, Missouri, USA), battery level (new batteries), and deployment duration. Camera traps were placed in March–April 2019 for a period of two to three months until June–July 2019, making sure that the period of camera trapping was always the same for all three placement types in a grid cell. We chose a short period in spring as previous data from the SCANDCAM project suggested the highest detection probability for large carnivores was in spring (unpublished data), while maintaining a short period in order to conform to the closure assumption of occupancy models as much as possible (Mackenzie and Royle 2005). The closure assumption states that occupancy is constant over the study period, and therefore, there should be no migration or other changes in spatial distribution of a species over the study period. We could not standardize CT height and angle for all CTs as the lynx-targeted CTs were already placed. Therefore, we made sure that each trio of CTs had the same height and angle

and were aimed in the same compass direction, to enable comparison among placements within each grid cell. Habitat-patch and landscape-scale random CTs were placed on the tree nearest to the randomly generated location with a good visibility (at least 5 m in front of the CT) in the correct compass direction. All CTs were set to take a time-lapse image at 8:00 a.m. local time, in addition to being activated by an animal passing, to enable checking of CT functioning and visibility.

A deep convolutional neural network trained with previous images from the SCANDCAM project was used to classify all images using TensorFlow (Abadi et al. 2016). The workflow included a two-step approach, where a pre-trained Faster R-CNN network (Ren et al. 2015) was used to split the images into multiple objects (such as animals, humans, or vehicles), followed by an Inception-ResNet v2 network (Szegedy et al. 2016) to classify the objects identified as animals to species. For all images, the software suggested a species identity with a given probability. This workflow was integrated in a data management system that aggregated images into events and defined an observation event as an image or a series of images taken with a time span of five minutes both prior to and after the series of images. A group of staff and students from the Norwegian Institute for Nature Research (NINA) verified all species identifications. All images of humans and vehicles were removed in order to conform to Norwegian privacy regulations, but we retained information of their passing.

Covariates

At the landscape scale, we calculated the mean elevation (elevation), percentage of forest cover (forest.grid), and percentage of field cover (field.grid) for each 50-km^2 grid cell based on data with a 1 km^2 spatial resolution collected by Bouyer et al. (2015a). We included these parameters as they characterized differences in our study area on a landscape scale, including the gradient from river valleys with agricultural fields in the west to forests in the east and higher hills in the northeast (Fig. 1). We did not include more species-specific covariates at this scale, as our main interest was in the factors affecting detection probability of the different species and study designs.

At the habitat-patch scale, we calculated the percentage of forest cover (forest.site) and

percentage of field cover (field.site) in a 1 km² circular buffer around each CT based on the same data as for the landscape scale, as general descriptors of the habitat surrounding each CT. We also included the terrain ruggedness index (ruggedness) at the CT site based on a digital elevation model of 10 m spatial resolution (Kartverket, Hønefoss, Norway) to correct for its potential effects on site use of the different species. We included this parameter as the targeted CTs were often placed in sites with high ruggedness as these are often selected by resting lynx (Bouyer et al. 2015b). Lastly, we included a dummy variable (target.site) that indicated if the CT was located in a selected habitat patch (1 for the targeted and habitat-patch CTs) or not (0 for the landscape CTs).

At the microsite scale, as lynx-targeted CTs were placed in different microsites we included this parameter (microsite) as a variable determining detection probability. Based on the presence in the field of view of the CT within the detection zone, microsites were classified when deploying the CTs as: (1) no visible feature, (2) forest road (either used or not), (3) wildlife trail, or (4) cliff/boulder (when the CT was aimed at a cliff face or large boulder). Most targeted CTs were placed in a specific microsite (15 on a forest road, 9 on a wildlife trail, 6 next to a cliff/boulder, and 8 at no visible feature) whereas most random CTs of both types were placed at microsites with no visible feature (3 on a wildlife trail, 5 next to a cliff, and 68 at no feature). Targeted CTs where no visible feature was present when visiting the CT were likely aimed at a site where the responsible volunteer had previously seen lynx tracks.

To correct for differences in visibility in front of the CT that might influence the effectivity of the PIR sensor, we estimated the maximum distance at which each CT detected a human based on the walk test function of the CTs (visibility). Furthermore, we included the height of the CT (cam.-height) as a covariate on the detection probability.

We standardized (scaled) all continuous covariates by subtracting the mean and dividing by one standard deviation (mean, standard deviation, and range of the unscaled covariates are given in Appendix S1: Table S1). Within each hierarchical level in the model, we reduce issues with collinearity by making sure that Pearson correlation coefficients for all pairs of covariates were below 0.6 and variance inflation factors below 3 (Zuur et al. 2010).

Sampling of the datasets to mimic different study designs

To test how the number of CTs influences detection probability and therefore the precision of occupancy probability estimates in a grid cell, we ran models on six (sub)sets of data: (1) the full dataset, (2) the targeted and landscape CTs, (3) the targeted and habitat-patch CTs, (4) the habitat-patch and landscape CTs, (5) the targeted CTs, and (6) the landscape CTs. We did this to compare the effects of targeting the CT (targeted versus random), different numbers of CTs (3, 2, or 1) as well as different spread of the CTs over the grid cell, comparing a spread out approach (targeted + landscape, and habitat-patch + landscape) that should in theory give a better sampling of the area, and the more regularly used combination of several CTs with short inter-camera distance (targeted + habitat-patch). Furthermore, this allowed us to compare the results from using a single targeted CT with a single random CT per grid cell.

Modeling framework

For all subsets including more than one CT per grid cell, we used multi-scale occupancy models as described by Mordecai et al. (2011) and Kéry and Royle (2016). We composed the state process model using two equations, starting with the occupancy state (ψ_i) of each 50-km² grid cell i:

$$z_i \sim \text{Bernoulli}(\psi_i), \qquad (1)$$

where z_i represents the observed occupancy state in grid cell i, followed by the site use ($\theta_{i,j}$) of a CT site j in grid cell i, which is conditional on the respective occupancy state:

$$a_{i,j}|z_i \sim \text{Bernoulli}(z_i \times \theta_{i,j}). \qquad (2)$$

where $a_{i,j}$ represents the observed site-use state at CT site j in grid cell i. This enabled us to estimate (1) the probability of occupancy in each grid cell, (2) the effect of covariates on site-use probability, and (3) compare site-use probability estimates among CT placement types (1 to j) within grid cells, assuming that species that occupy grid cell i were available for detection by all CTs in that cell. We interpret site-use as the probability of a species using the direct surroundings of a CT site

as for a point estimate, as often done for single CT occupancy models (sensu Steenweg et al. 2018), instead of the probability of a species using the very small patch of habitat in the field of view of the CT (sensu Evans et al. 2019).

The observation model, which is conditional on the state of use is then denoted as:

$$y_{i,j,k}|a_{i,j} \sim \text{Bernoulli}(a_{i,j} \times p_{i,j,k}), \qquad (3)$$

where $p_{i,j,k}$ is the probability of detecting the species given use of site j. $y_{i,j,k}$ is the detection or non-detection of a species during the kth period at CT site j in grid cell i. Detection occasions were pooled into 5-day periods, as is common in camera-trapping studies of mobile species (Burton et al. 2015).

We ran single-species models to accommodate different effects of CT placement on the detectability of different species and modeled occupancy (landscape scale), site use (habitat scale) and detection (microsite/CT scale) using the following series of logistic regression equations:

$$\begin{aligned}\text{logit}(\psi_i) = {} & \alpha_0 + w_1 \times \alpha_1 \times \text{elevation}_i + w_2 \times \alpha_2 \\ & \times \text{forest.grid}_i + w_3 \times \alpha_3 \times \text{field.grid}_i\end{aligned}$$
$$(4)$$

$$\begin{aligned}\text{logit}(\theta_{i,j}) = {} & \beta_0 + w_4 \times \beta_1 \times \text{target.site}_{i,j} + w_5 \\ & \times \beta_2 \times \text{ruggedness}_{i,j} + w_6 \times \beta_3 \\ & \times \text{forest.site}_{i,j} + w_7 \times \beta_4 \\ & \times \text{field.site}_{i,j}\end{aligned}$$
$$(5)$$

$$\begin{aligned}\text{logit}(p_{i,j,k}) = {} & \delta_{0j} + \delta_1 \times \text{microsite}_{i,j} + \delta_2 \\ & \times \text{cam.height}_{i,j} + \delta_3 \times \text{visibility}_{i,j}.\end{aligned}$$
$$(6)$$

We calculated a single estimate for the intercept of both state parameters indicating the average occupancy (α_0) and the average site-use probability (β_0) of the species in the whole study area, respectively. We included an intercept per placement type j to enable the estimation of an average detection probability (δ_{0j}) per placement type per species after correction for the different covariates. Parameters α_1–α_3, β_1–β_4, and δ_1–δ_3 represent the slopes for the different covariates. w_1–w_7 represent Bayesian inclusion parameters, used to evaluate the level of support for each

covariate (Kuo and Mallick 1998). w_4 was set to zero for the subset using only the targeted and habitat-patch CT as the target.site$_{i,j}$ covariate was the same for both placement types.

For the two subsets that only included a single CT per grid cell, we used conventional occupancy models (MacKenzie et al. 2002) that only included a single scale for the state model (formula 1) and an observation model, which is conditional on the occupancy state, and is then denoted as:

$$y_{i,k}|z_i \sim \text{Bernoulli}(z_i \times p_{i,k}), \qquad (7)$$

where $p_{i,k}$ is the probability of detecting the species given occupancy in grid cell i. $y_{i,k}$ is the detection or non-detection of a species during the kth period at the single CT in grid cell i.

Due to the lack of differentiation between site use and occupancy for the single-CT models, and the use of only one placement type in each model, we used the following series of logistic regression equations for the two subsets including only one CT per grid cell:

$$\begin{aligned}\text{logit}(\psi_i) = {} & \alpha_0 + w_1 \times \alpha_1 \times \text{elevation}_i + w_2 \times \alpha_2 \\ & \times \text{forest.grid}_i + w_3 \times \alpha_3 \times \text{field.grid}_i \\ & + w_4 \times \alpha_4 \times \text{ruggedness}_i + w_5 \times \alpha_5 \\ & \times \text{forest.site}_i + w_6 \times \alpha_6 \times \text{field.site}_i\end{aligned}$$
$$(8)$$

$$\begin{aligned}\text{logit}(p_{i,k}) = {} & \delta_0 + \delta_1 \times \text{microsite}_i + \delta_2 \\ & \times \text{cam.height}_i + \delta_3 \times \text{visibility}_i.\end{aligned}$$
$$(9)$$

For each species and dataset combination, we estimated posterior distributions using Markov chain Monte Carlo (MCMC) implemented in JAGS (version 4.3.0, Plummer 2003) called from R (version 4.0.0, R Core Team 2020) using the jagsUI package (version 1.5.1, Kellner 2019). Inclusion parameters (w_c) were Bernoulli distributed with a prior probability of 0.5. Thus, these parameters could switch to 0 or 1 for each iteration, determining if each covariate is included in that iteration or not. We first ran a full model including all covariates including inclusion parameters (formulae 4–6 and formulae 8–9) and selected covariates when $w_c \geq 0.6$. We then ran a final model for each species and dataset combination including only those

selected covariates. We used the final model including the full dataset (all three placement types) to explore effects of placement type and covariates on detection probability and all final models for the comparison among subsets of the data. We interpreted the results from the dataset including all three CTs as the least biased estimate of all parameters and of which covariates were most important. Therefore, we used the observed proportion of grid cells where the species was detected in the full dataset as a baseline minimum estimate of known occupancy for all species, from here on referred to as known minimum occupancy. For comparison of detection probabilities among the different subsets with multiple CTs, we calculated a combined detection probability for the combination of CTs by multiplying the intercepts of the detection probabilities of each placement type for a subset of 1 000 iterations from the posterior distributions.

We used vague priors for all parameters, a uniform distribution from 0 to 1 for all intercepts (before logit transformation) and a normal distribution with a mean of 0 and a precision of 0.01 for all slopes. We provided an initial value of zero for the intercept and all covariate slopes of the occupancy part of the model. We ran the models with Bayesian inclusion parameter for 50,000 iterations (+50,000 iterations for burn-in), and the final models for 30,000 iterations (+20,000 iterations for burn-in), all thinned by 10 on three chains. We assessed model convergence using the Gelman-Rubin convergence statistic (R) and trace plots (Brooks and Gelman 1998). We present the median and 89% credible interval (McElreath 2020) estimated using the highest density interval (HDI) as included in the bayestestR package (Makowski et al. 2019) for all parameters, and interpret non-overlapping HDIs as convincing evidence for a difference between estimates (Schenker and Gentleman 2001). All code and data used in the analyses are provided on GitHub (https://github.com/Tim-Hofmeester/camera-placement).

RESULTS

We deployed 114 camera traps (38 lynx-targeted CTs, 38 random CTs within the same habitat patch, and 38 random CTs within the same 50-km^2 grid cell, Fig. 1) for a total of 9715

Table 1. Number of observation events and camera trap (CT) sites with observations (within brackets) per placement type and naïve occupancy at 50-km^2 grid-cell level for each species.

Species	Lynx-targeted CT	Habitat-patch CT	Landscape CT	Naïve occupancy
Brown bear	0 (0)	0 (0)	1 (1)	0.03
Wolf	13 (5)	1 (1)	3 (2)	0.13
Lynx	11 (3)	0 (0)	1 (1)	0.08
Wolverine	7 (5)	1 (1)	2 (2)	0.21
Badger	18 (5)	5 (2)	3 (3)	0.13
Red fox	97 (27)	26 (15)	12 (7)	0.92
Pine marten	5 (5)	4 (3)	3 (3)	0.24
Stoat	1 (1)	0 (0)	0 (0)	0.03
Moose	132 (25)	93 (23)	81 (20)	0.92
Red deer	3 (3)	9 (2)	8 (3)	0.18
Roe deer	293 (23)	126 (20)	43 (9)	0.71
Mountain hare	222 (30)	94 (23)	76 (23)	0.95
Red squirrel	13 (5)	4 (2)	0 (0)	0.13

trap nights and photo-captured 13 mammal species of which eight were carnivores. In order of size (largest to smallest), we photographed the following carnivore species: brown bear (one CT site), wolf (eight CT sites), lynx (four CT sites), wolverine (eight CT sites), badger (10 CT sites), red fox (49 CT sites), pine marten (11 CT sites), and stoat (*Mustela erminea*; one CT site; Table 1). Other mammal species that we captured were (largest to smallest): moose (68 CT sites), red deer (*Cervus elaphus*; eight CT sites), roe deer (52 CT sites), mountain hare (76 CT sites), and Eurasian red squirrel (*Sciurus vulgaris*; seven CT sites; Table 1). For all species, except brown bear (only one record) and red deer, we recorded most events on the targeted CTs (Table 1).

We had sufficient detections (>10) at all placement types (targeted, habitat-patch, and landscape CTs) to perform the full analysis including all data subsets for four species: moose, roe deer, red fox, and mountain hare (Table 2). Four other species, wolf, lynx, badger, and red squirrel, only had sufficient detections (>10) at the targeted CT sites, so we only performed a single analysis on these species using the data from targeted CTs (Table 2). All models converged with $\hat{R} < 1.1$.

Table 2. Summary of the selected models for each species and dataset combination.

Species	All cameras†	Targeted + landscape†	Targeted + habitat patch†	Habitat patch + landscape†	Targeted†	Landscape†
Herbivores						
Moose	ψ(.)θ(Fld.s) p(full)	ψ(.)θ(.) p(full)	ψ(.)θ(Fld.s) p(full)	ψ(.)θ(.) p(full)	ψ(Rug) p(full)	ψ(Frs.s) p(full)
Roe deer	ψ(.)θ(Fld.s) p(full)	ψ(.)θ(Fld.s) p(full)	ψ(.)θ(Fld.s) p(full)	ψ(.)θ(Fld.s) p(full)	ψ(.)p(full)	ψ(.)p(full)
Mountain hare	ψ(.)θ(.) p(full)	ψ(.)θ(.) p(full)	ψ(.)θ(.) p(full)	ψ(.)θ(.) p(full)	ψ(.)p(full)	ψ(.)p(full)
Red squirrel	-	-	-	-	ψ(Frs.g + Fld.g + Frs.s)p (full)	-
Carnivores						
Wolf	-	-	-	-	ψ(.)p(full)	-
Lynx	-	-	-	-	ψ(Ele) p(full)	-
Badger	-	-	-	-	ψ(.)p(full)	-
Red fox	ψ(.)θ(Trg.s) p(full)	ψ(.)θ(Trg.s) p(full)	ψ(.)θ(.) p(full)	ψ(.)θ(.) p(full)	ψ(.)p(full)	ψ(Fld.g + Rug)p (full)

† Models including only covariates with a Bayesian inclusion parameter (w_c) higher than 0.6. Model parameter abbreviations are ψ, occupancy probability; θ, site-use probability; and p, detection probability. Model covariate abbreviations are Ele, Elevation; Frs.g, Forest.grid; Fld.g, Field.grid; Trg.s, Target.site; Rug, Ruggedness; Frs.s, Forest.site; Fld.s, Field.site. A dot (.) shows that no covariates were included in that part of the model. All models included a set of three covariates (full) on detection probability, microsite, camera height, and visibility. See main text and Appendix S1: Table S5 for further description and coefficient estimates of the covariates.

Factors affecting detection probability

We used the full dataset to compare detection probabilities among the three CT placement types, as well as to test for the influence of several covariates for the four most common species. As noted before, we interpret detection probabilities among placement types as different if they had non-overlapping 89% credible intervals (measured as highest density interval—HDI). Comparing the intercepts for the three placement types, indicating differences among placement types after correction for the studied covariates, roe deer, red fox, and mountain hare had the highest detection probability on lynx-targeted CTs (Fig. 2, Appendix S1: Table S2). In contrast, moose had very similar detection probabilities for all three CT-placement types. Detection probability of roe deer was different for all three placement types, highest for the targeted CT, intermediate for the habitat-patch CT, and lowest for the landscape CT. For red fox, detection probability was higher for the targeted CT than for the habitat-patch CT. Detection probability of mountain hare was higher for the targeted CT compared to the landscape CT (Fig. 2, Appendix S1: Table S2).

We found effects of camera-trap level covariates on detection probability for all species (Fig. 3, Appendix S1: Table S3). Detection probability of moose was higher on forest roads compared to CTs aimed at cliff sides or boulders. For roe deer, detection probability increased with visibility and was lower on wildlife trails and CTs aimed at cliff sides and boulders compared to CTs with no visible feature. Detection probability of red fox increased with CT height, decreased with visibility and was lower on wildlife trails compared to sites without visible feature. Mountain hare detection probability decreased with visibility (Fig. 3, Appendix S1: Table S3).

Despite detection probabilities at the random CTs being so low that we could not run a complete analysis, we found similar detection probabilities at targeted CTs for wolf, lynx, and badger as for moose, roe deer, red fox, and mountain hare, but with wider 89% HDIs (Appendix S1: Table S4). Where none of the covariates explained variation in wolf detection probability, we did find effects of several covariates for the other species (Table 3). Lynx detection probability increased with CT height and decreased with visibility. Badger detection probability was lower on forest roads compared to CTs aimed at no visible feature and decreased with CT height.
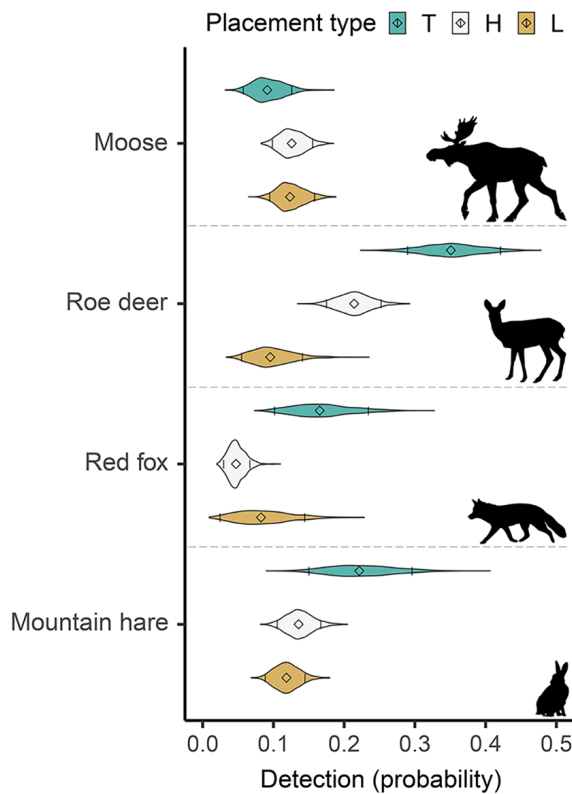
Fig. 2. Violin plot of the posterior distributions of the back-transformed intercepts of detection probability for each of the three placement types from the multi-scale models on the full dataset including all selected covariates for moose, roe deer, red fox and mountain hare, ranked by body mass (from top to bottom). Abbreviations are T, the targeted camera trap (CT); H, the random habitat-patch CT; and L, the random landscape CT. Diamonds indicated the median and vertical bars the upper and lower limit of the 89% credible interval (highest density interval). Species silhouettes are drawn by T. Hofmeester except for moose (by X. Giroux-Bougard) and red fox (by F. Sayol), CC0 1.0, as provided by www.phylopic.org.

Similarly, detection probability of red squirrel was also lower on forest roads compared to CTs without visible feature and decreased with visibility (Table 3).

Covariates influencing occupancy and site use

Considering all CTs, site-use probability of both moose ($\beta_{4,all}$ = 1.5, 89% HDI = 0.13–3.5) and roe deer ($\beta_{4,all}$ = 4.2, 89% HDI = 1.4–7.4) increased with the percentage of fields in the
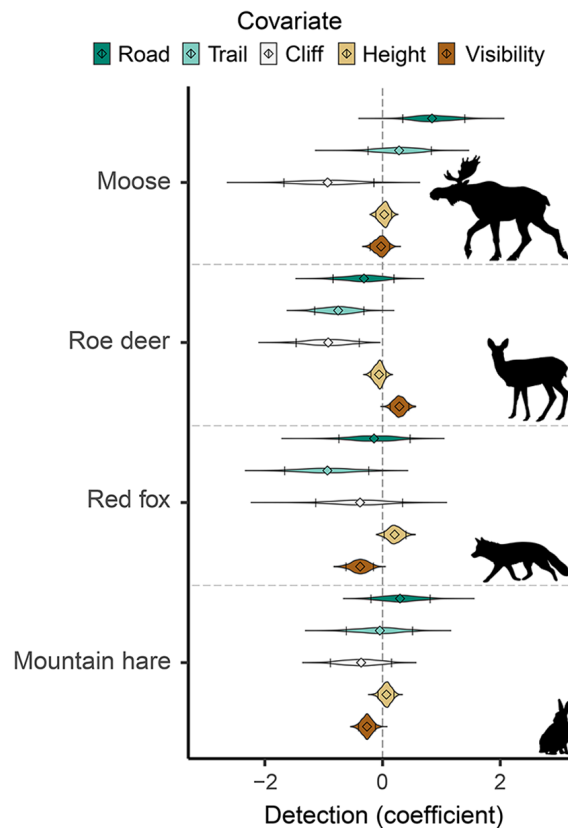

Fig. 3. Violin plot of the posterior distributions of the slopes of all covariates for detection probability from the multi-scale models on the full dataset including all selected covariates for moose, roe deer, red fox and mountain hare, ranked by body mass (from top to bottom). Abbreviations are road, forest road microsite; trail, wildlife trail microsite; cliff, camera traps (CTs) aimed at cliff sides or large boulders; height, CT height; and visibility, the visibility in front of the CT as measured using the walk test. Estimates of microsite categories are relative to placement at a microsite with no visible feature. Diamonds indicated the median and vertical bars the upper and lower limit of the 89% credible interval (highest density interval). Species silhouettes are drawn by T. Hofmeester except for moose (by X. Giroux-Bougard) and red fox (by F. Sayol), CC0 1.0, as provided by www.phylopic.org.

direct surroundings (1 km^2) of the CT (Appendix S1: Table S5). Red fox had a higher site-use probability at the targeted habitat patch (targeted and habitat-patch CTs) compared to the habitat patch with the landscape CT ($\beta_{1,all}$ = 2.4, 89% HDI =-0.82–4.0).

Table 3. Estimates of the slopes of the covariates on detection probability relative to the intercept (placement on no feature with a mean value for camera height and visibility), including their 89% credible intervals (highest density interval), for the four species where we only ran a model on data from the targeted cameras, based on selected models.

Parameter	Detection (coefficient)
Wolf	
Forest road	0.37 (−2.9 to 3.5)
Wildlife trail	−7.5 (−22 to 2.1)
Cliff/Boulder	−6.4 (−20 to 9.2)
Camera height	−0.10 (−0.79 to 0.52)
Visibility	−0.22 (−2.1 to 1.6)
Lynx	
Forest road	−3.6 (−8.0 to 1.4)
Wildlife trail	−8.4 (−22 to 4.5)
Cliff/Boulder	−6.7 (−16 to 2.4)
Camera height	**3.7 (1.2 to 7.0)**
Visibility	**−3.5 (−7.8 to −0.36)**
Badger	
Forest road	**−6.4 (−13 to −0.47)**
Wildlife trail	−3.1 (−7.9 to 2.1)
Cliff/Boulder	−1.9 (−9.5 to 5.4)
Camera height	**−2.9 (−4.9 to −1.2)**
Visibility	−0.92 (−3.6 to 1.5)
Red squirrel	
Forest road	**−8.7 (−18 to −1.9)**
Wildlife trail	−0.67 (−2.5 to 1.2)
Cliff/Boulder	−0.41 (−2.2 to 1.5)
Camera height	−0.36 (−1.3 to 0.51)
Visibility	**−1.4 (−2.4 to −0.49)**

Note: Estimates in boldface have 89% credible intervals that do not include zero.

For the four species where we could only run single CT models using the targeted CTs, lynx occupancy probability decreased with elevation at the grid cell level ($\alpha_{1,T}$ = −2.8, 89% HDI = −7.1 to −0.75). Occupancy of red squirrel decreased with the percentage of forest cover in the grid cell ($\alpha_{2,T}$ = −10.3, 89% HDI = −18.4 to −3.8) and increased with the percentage of field cover in the grid cell ($\alpha_{3,T}$ = 8.8, 89% HDI = 2.0–16.2) and the percentage of forest cover in the direct surroundings of the CT ($\alpha_{5,T}$ = 8.0, 89% HDI = 2.6–13.8).

Effects of CT number and placement on detection probability and inferences on occupancy

When comparing the detection and occupancy probability estimates from selected models for the five datasets, all four common species had the highest detection probability for the model including three CTs (Fig. 4, Appendix S1: Table S2). The most precise occupancy estimate, as measured by the width of the 89% HDI, was obtained for the Targeted + Landscape CTs for moose and roe deer and for the full three CT set-up for red fox and mountain hare. Thus, the associations with covariates found for these models were interpreted as least biased. Moose showed very little variation among placement types, resulting in the number of CTs as the main determinant of detection probability estimates. Only combinations of two CTs that included the targeted CT resulted in occupancy estimates within the 89% HDI of the full dataset and with medians higher than the known minimum occupancy (Table 1, Appendix S1: Table S2). Occupancy estimates based on datasets with single CTs or two random CTs had lower precision (Fig. 4). Furthermore, single CT models found seemingly spurious associations with covariates that were not identified in the full three CT dataset (Table 2, Appendix S1: Table S5).

For roe deer, detection probability was highest for the full dataset, intermediate for all two CT combinations and targeted CTs, whereas the single landscape CT had the lowest detection probability close to zero (Fig. 4). All two CT datasets resulted in occupancy estimates that were within the 89% HDI of the full dataset and with medians higher than the known minimum occupancy (Table 1, Appendix S1: Table S2). Especially the occupancy estimate from the single landscape CT had a large credible interval (Fig. 4). The positive association of site use with the percentage of fields in a 1 km^2 circular buffer around the CT was similar for all multi CT models (Appendix S1: Table S5).

Detection probability of red fox was highest for all multi CT datasets including the targeted CT, intermediate for the single targeted CT and combination of two random CTs, and lowest for the landscape random CT, which was close to zero (Fig. 4). Combinations of two CTs including the targeted CT resulted in landscape-level occupancy estimates within the 89% HDI of the full dataset and with medians higher than the known minimum occupancy (Table 1, Appendix S1: Table S2). Datasets with single CTs or two random CTs underestimated occupancy and had
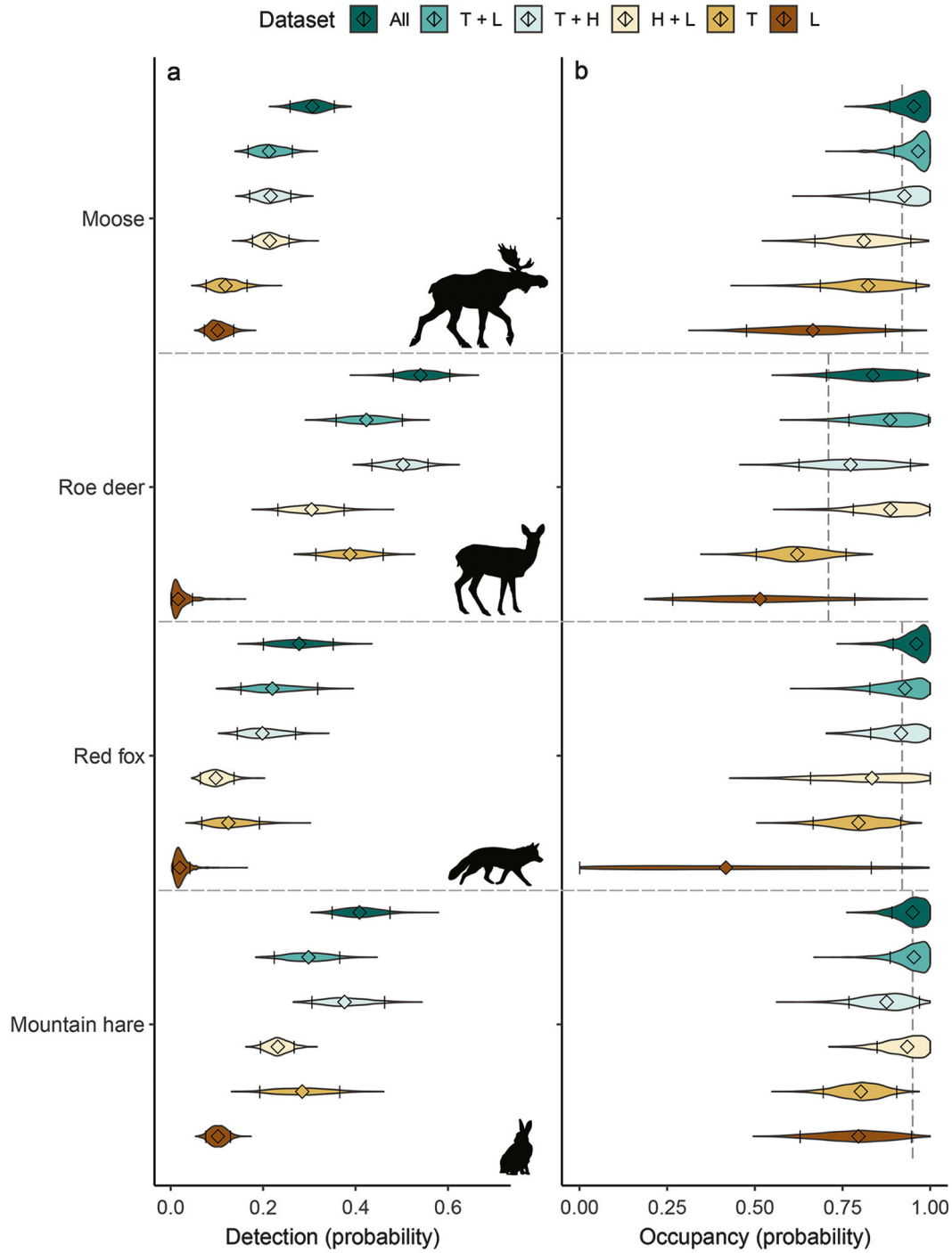
Fig. 4. Violin plot of the posterior distribution of detection probability (combined for all camera trap (CT) placement types) and occupancy probability at grid-cell level estimated using selected models for each of the subsets of data for moose, roe deer, red fox and mountain hare, ranked by body mass (from top to bottom). All = all three placement types, T + L = the targeted and random landscape CTs, T + H = the targeted and random habitat-patch CTs, H + L = the random habitat-patch and random landscape CTs, T = only the targeted CT, and

(Fig. 4. *Continued*)

L = only the random landscape CT. Diamonds indicated the median and vertical bars the upper and lower limit of the 89% credible interval (highest density interval). Naïve occupancy estimates based on all three CTs are presented as vertical dashed lines. Species silhouettes are drawn by T. Hofmeester except for moose (by X. Giroux-Bougard) and red fox (by F. Sayol), CC0 1.0, as provided by www.phylopic.org.

lower precision, with a very large 89% HDI using the single random landscape CT (Fig. 4). Furthermore, we found seemingly spurious associations with covariates in the dataset with the single random landscape CT that were not identified in the full three CT dataset (Table 2, Appendix S1: Table S5).

For mountain hare, differences among datasets in detection probability were similar as for roe deer, but with smaller differences among datasets and a higher detection probability for the random landscape CT (Fig. 4). Only the targeted + landscape datasets had occupancy estimates within the 89% HDI of the full dataset and a median higher than the known minimum occupancy, likely because of the very high minimum occupancy of 0.95 (Table 1, Appendix S1: Table S2). None of the datasets identified any associations of covariates with site use or occupancy (Table 2).

DISCUSSION

Camera-trapping studies often target certain species by placing CTs in particular settings to maximize detection of that species, whereas the relatively unselective PIR sensor of CTs detects a whole range of species. In addition to targeting CTs, researchers can also use multiple CTs at individual sampling sites to increase detection probabilities. In this study, we tested how the targeted placement of CTs aimed at Eurasian lynx, as placed by volunteers in a community science program, and the number of CTs influenced detection probability for non-target mammals in a boreal forest region in southeast Norway. We found higher numbers of detections and higher detection probabilities at lynx-targeted CTs for all studied species except moose and red deer. Moose detection was similar for lynx-targeted and non-targeted CTs. Red deer had fewer detections at lynx-targeted CTs but based on so few records that we deem the red deer estimate as

very unreliable. Several studies investigating the detection of species on and off trails have found similar results, where for most species, detection probabilities were either highest on trails or not different between on or off trail placements (Cusack et al. 2015, Kolowski and Forrester 2017, Reilly et al. 2017, Fonteyn et al., 2021). In contrast, Harmsen et al. (2010) found a negative association for a prey species (brocket deer; *Mazama americana*) on CTs targeted toward jaguars (*Panthera onca*), while they found positive associations for other carnivore species. Similar habitat use by different carnivore species could explain the higher number of detections and detection probabilities of other carnivores, such as wolves, red foxes, and badgers, on lynx-targeted CTs. However, we also found higher detection probabilities of roe deer and mountain hares, frequent prey of Eurasian lynx in the area (Odden et al. 2006), on lynx-targeted CTs. We think this could potentially be caused by two, non-mutually exclusive, mechanisms. First, as all our targeted CT sites are selected by volunteers based on their experience of seeing lynx tracks or places where they would expect lynx, it could be that volunteers placed CTs in places where they saw roe deer and/or mountain hare tracks as they know these are important prey species. Second, because of the low environmental productivity, all mammal species have relatively large home and day ranges in boreal forests (Morellet et al. 2013, Duncan et al. 2015), meaning they have to move over large distances on a regular basis. Therefore, all species might select for the same efficient travel routes when moving through the landscape, searching for the paths of least resistance. In this landscape, this ease of movement may provide a large benefit that outweighs the relatively low risk caused by the overall low densities of carnivores. Either way, the relatively high detection probability of most species at lynx-targeted CTs in our study indicates that these CTs can be used to study occupancy of

non-target species in our, and similar, boreal systems.

Camera-trap data are often analyzed using occupancy models (Burton et al. 2015, Sollmann 2018) and it has been suggested that the occupancy probability as derived from single CTs should be interpreted as a measure of site use rather than occurrence (e.g., Neilson et al. 2018, Steenweg et al. 2018), especially when used in continuous habitat (Efford and Dawson 2012). Nevertheless, designs estimating occupancy at predefined grid cells using single CTs are still relatively common. This is likely because a design to estimate occupancy at predefined grid cells links better to grid-based monitoring methods that are often used for other species groups (Stevens 1997) and allows for easier extrapolation of estimates to a wider landscape. Additionally, it makes the area that is sampled explicit. However, we found that using one CT per grid cell, even if it was targeted, resulted in underestimates of occupancy, which did not overlap with the 89% HDI of a three CT model and were lower than the known minimum occupancy. Single random CTs resulted in too few records for all but four species to run analyses. For two of those four species, red fox and roe deer, detection probabilities on single random CTs were so low that occupancy estimates became very imprecise. This is likely because CTs sample points (Efford and Dawson 2012, Steenweg et al. 2018) and are thus influenced by the (micro)habitat of that point, especially if a single point is used to sample a larger grid cell. In other words, a single point is likely to under sample the available (micro)habitats in a grid cell in comparison to, for example, a design based on line transects, which by design samples multiple (micro)habitats. We would thus recommend the use of multiple CTs per grid cell to increase detection probabilities in grid-based designs by better sampling the available habitat in the grid cell, similar to what is often already done in site-based designs using random CT placement (Kays et al. 2020).

In line with several recent studies, we found that, as an alternative to targeting CT placement, adding one or multiple CTs per site also improved detection probabilities and the accuracy of the occupancy estimate (Pease et al. 2016, Evans et al. 2019, Wong et al. 2019). A potential mechanism explaining the increased detection probability when using multiple CTs is that this increases the chance that one of the CTs is located in a site that is used by the species. Many animal characteristics can determine the use of a specific site, determining the probability of that species walking past a CT and thus if the species is available for detection (Hofmeester et al. 2019). Based on this mechanism, one would expect interspecific differences in the response of detection probability to an increased number of CTs and that these differences could potentially be explained by local site characteristics. We did indeed find that the effects of additional CTs on detection probability were placement and species specific, similar to previous studies (Pease et al. 2016, Evans et al. 2019, Wong et al. 2019). For example, the addition of random CTs hardly resulted in extra detections of large carnivores such as lynx and wolf. Thus, using multiple CTs to increase detection probabilities can still lead to species-specific biases depending on the site characteristics of the CT locations.

Our study confirms an increasing body of work showing that microsite characteristics, whether measurable with covariates or not, have a large influence on detection probabilities of species on CTs (Kolowski and Forrester 2017, Evans et al. 2019, Kolowski et al. 2021). Several species had different detection probabilities at microsites that were defined by different features (forest roads, wildlife trails, or cliff sides), likely due to differences among species in their microsite selection. For example, moose often select forest roads for movement and foraging (Loosen et al. 2021), whereas these might be avoided by red squirrels to reduce predation (Andrén and Delin 1994). We also found contrasting results across species of the effects of visibility in front of the CT on detection probabilities. These are also likely related to differences in habitat selection and movement strategy among the species (Kolowski et al. 2021) rather than differences in PIR-sensor sensitivity (Rowcliffe et al. 2011, Hofmeester et al. 2017). Movement of lynx, red foxes, mountain hares, and red squirrels, as predators and small prey, are more channeled toward sites with a short line of sight (many obstructions) compared to roe deer, which could explain the contrasting patterns we found between these species. As, to date, relatively few studies have investigated the effect of movement on detection

by CTs (but see, e.g., Stewart et al. 2018), we suggest that studies that simultaneously investigate movement patterns, using snow tracking or GPS collars, and CTs are needed to disentangle the effect of movement on detection.

Relatively little attention has been given to the potential effect of the number of CTs used in a site and habitat associations found in occupancy models. For two species, red fox and moose, single CTs resulted in associations with covariates that were not present in any of the multi-CT models. This indicates that these are likely spurious associations. Because of this, we suggest that the found associations at single targeted CTs for lynx and red squirrel should also be interpreted with care. These findings are consistent with the effect of the number of CTs on apparent associations with covariates reported by Pease et al. (2016). We thus want to underline that the number of CTs per site can influence the interpretation of associations between occupancy and habitat covariates and that consequently; wildlife–habitat associations at large scales based on a single CT per site should be interpreted with care.

The grid size used for CT spacing and grid cell-based occupancy estimates in our study was relatively large compared to most other CT studies where a spacing of 1–2 km is fairly common (e.g., Tobler et al. 2008, Rovero et al. 2014). One of the studies on which we based the lynx-targeted design used a similar approach but with grid cells of 7.3 km^2 to estimate the density of a Swiss lynx population (Zimmermann et al. 2013). However, their total study area with multiple lynx individuals was 760 km^2, which is smaller than the average female lynx home range (930 km^2) in Norway (Bouyer et al. 2015a). Therefore, we decided to increase the size of our grid cells to 50 km^2 to cover the much larger home ranges of lynx in our study system and enable the capture of multiple lynx with the same number of CTs. As most of our non-target species also likely occur at low densities, with relatively large home ranges, this large grid size might be appropriate for those species as well. However, the species that we studied vary widely in home range size, from several hectares for red squirrel, to several square kilometers for mountain hare and pine marten to hundreds to thousands of square kilometers for wolverine,

wolves, and lynx (Andrén and Delin 1994, Mattisson et al. 2013, Bouyer et al. 2015a). As the interpretation of occupancy results is determined by home range size of the studied species (Efford and Dawson 2012, Steenweg et al. 2018), the 50-km^2 grid cell landscape scale should be interpreted differently for the different species. For species with a home range smaller than 50 km^2, occupancy can be interpreted as fitting to the 2nd order of habitat selection (Johnson, 1980) and interpreted as occurrence in a grid cell. However, for all species with a home range larger than 50 km^2, occupancy should be interpreted as fitting to the 3rd order of habitat selection (Johnson, 1980) and thus be interpreted as site use or occupancy of that part of the home range (Efford and Dawson 2012). Despite the many disadvantages of studying species at low densities, one of the advantages is that the relationship between population density and occupancy is more linear at low densities, enabling the tracking of population trends using occupancy models (Steenweg et al. 2018).

Despite our effort, we had a relatively low number of detections for several species in our analyses and insufficient data for several species to perform analyses. Even two common species, roe deer and red fox, had such low detection probabilities on single random CTs that the precision of their occupancy estimates became too low to be of use for studies interested in this parameter. This is likely a result of relatively low densities of most species in the study area (due to a combination of the boreal nature of the ecosystem and harvest management of all the studied species). Unfortunately, we did not have sufficient records of red deer to perform analyses, as this was the single species showing less detections at the targeted CT compared to either random CT. This could be due to the relatively low densities and recent recolonization of the study area by red deer (Rosvold et al. 2012). Wolverines and bears also had too few records for statistical analysis. Regarding the target species of our monitoring program, Eurasian lynx, the targeted CTs were responsible for all but one record, underlining the practical need of this targeted placement for this species, especially as the very low densities result in few records even on targeted CTs. Overall, we detected all forest-dwelling and fully terrestrial mammal species

known to occur in the area. Within the study ecosystem, species with more specialized (aquatic) habitat use, such as Eurasian beaver (*Castor fiber*) and Eurasian otter (*Lutra lutra*), are also present but were not detected by any CT. Similarly, the CTs did not detect any mammals smaller than a stoat. It is therefore important to realize, and explicitly state, the limitations of any study's ability to detect the full mammal community structure.

Community science projects are often criticized for a lack of focus on data quality (Lukyanenko et al. 2016). Camera traps have been suggested as a good tool for community science as they enable the recording of effort and collect pictures that can be used to verify species identification (McShea et al. 2016, Forrester et al. 2017). The lack of standardization when placing CTs could, however, still be an issue. The targeted CTs in our study were all placed by volunteers in a long-term scheme designed to monitor Eurasian lynx. Although volunteers placed CTs in a variety of microsites, this variation could be included in the statistical modeling. In this way, we were able to correct for potential differences in detection among microsites after which the targeting led to the highest detection probability for most species. Furthermore, the involvement of hunters as volunteers in lynx monitoring continues efforts to lower conflict levels by engaging in co-generation of the knowledge base for wildlife management (Skogen 2003). This underlines that any study design will inevitably have to trade-off multiple objectives (economic, social, and ecological). The key issue that our analysis underlines is the need to be aware of the consequent effects this has on the data and to, where possible, correct for biases in a statistical framework.

CONCLUSIONS

In this study, we found that most species in a boreal mammal assemblage, including carnivores and their prey, had the highest detection probability at lynx-targeted CTs. Furthermore, two CTs, one targeted, and one randomly placed, generally resulted in estimates of occupancy in 50-km^2 grid cells as accurate and precise as three CTs, whereas single CTs underestimated occupancy at the grid-cell level often below the known minimum occupancy as determined by

three CTs. Therefore, we recommend the use of at least two CTs, including at least one targeted CT, preferentially placed in different (micro)habitats, to survey occupancy in grid cells. This targeting should be aimed at microsites that are used by moving animals such as forest roads and wildlife trails. As detection probability was highest at targeted CTs for all analyzed species, having multiple targeted CTs in each grid cell would result in the best occupancy estimates. When using single CTs, we recommend to interpret occupancy as site use of an, as yet undefined, area directly surrounding the CT (Efford and Dawson 2012, Steenweg et al. 2018). The size of this area is a function of home range size and movement rates (Efford and Dawson 2012, Stewart et al. 2018) and therefore both species and site specific. We identify the need for more studies using a similar design in areas with other mammal communities, preferably in higher densities, to better inform future monitoring efforts aimed at monitoring population fluctuations of whole communities.

ACKNOWLEDGMENTS

LITERATURE CITED

Abadi, M., et al. 2016. TensorFlow: a system for large-scale machine learning. Pages 265–283 *in* Proceedings of the 12th USENIX conference on Operating Systems Design and Implementation. USENIX Association, Savannah, Georgia, USA.

Andrén, H., A. Delin, and H. Andren. 1994. Habitat selection in the Eurasian Red Squirrel, *Sciurus vulgaris*, in relation to forest fragmentation. Oikos 70:43–48.

Bouyer, Y., V. Gervasi, P. Poncin, R. C. Beudels-Jamar, J. Odden, and J. D. C. Linnell. 2015*a*. Tolerance to anthropogenic disturbance by a large carnivore: the case of Eurasian lynx in south-eastern Norway. Animal Conservation 18:271–278.

Bouyer, Y., G. San Martin, P. Poncin, R. C. Beudels-Jamar, J. Odden, and J. D. C. Linnell. 2015*b*. Eurasian lynx habitat selection in human-modified landscape in Norway: effects of different human habitat modifications and behavioral states. Biological Conservation 191:291–299.

Brooks, S. P., and A. Gelman. 1998. General methods for monitoring convergence of iterative simulations. Journal of Computational and Graphical Statistics 7:434–455.

Burton, A. C., E. Neilson, D. Moreira, A. Ladle, R. Steenweg, J. T. Fisher, E. Bayne, and S. Boutin. 2015. Wildlife camera trapping: a review and recommendations for linking surveys to ecological processes. Journal of Applied Ecology 52:675–685.

Cusack, J. J., A. J. Dickman, J. M. Rowcliffe, C. Carbone, D. W. Macdonald, and T. Coulson. 2015. Random versus game trail-based camera trap placement strategy for monitoring terrestrial mammal communities. PLOS ONE 10:e0126373.

Davis, A. J., R. McCreary, J. Psiropoulos, G. Brennan, T. Cox, A. Partin, and K. M. Pepin. 2018. Quantifying site-level usage and certainty of absence for an invasive species through occupancy analysis of camera-trap data. Biological Invasions 20:877–890.

Duncan, C., E. B. Nilsen, J. D. C. Linnell, and N. Pettorelli. 2015. Life-history attributes and resource dynamics determine intraspecific home-range sizes in Carnivora. Remote Sensing in Ecology and Conservation 1:39–50.

Efford, M. G., and D. K. Dawson. 2012. Occupancy in continuous habitat. Ecosphere 3:1–15.

Evans, B. E., C. E. Mosby, and A. Mortelliti. 2019. Assessing arrays of multiple trail cameras to detect North American mammals. PLOS ONE 14: e0217543.

Fonteyn, D., C. Vermeulen, N. Deflandre, D. Cornelis, S. Lhoest, F. G. A. Houngbégnon, J.-L. Doucet, and A. Fayolle. 2021. Wildlife trail or systematic? Camera trap placement has little effect on estimates of mammal diversity in a tropical forest in Gabon. Remote Sensing in Ecology and Conservation 7:321–336.

Forrester, T. D., M. Baker, R. Costello, R. Kays, A. W. Parsons, and W. J. McShea. 2017. Creating advocates for mammal conservation through citizen science. Biological Conservation 208:98–105.

Gimenez, O., S. Gatti, C. Duchamp, E. Germain, A. Laurent, F. Zimmermann, and E. Marboutin. 2019. Spatial density estimates of Eurasian lynx (*Lynx lynx*) in the French Jura and Vosges Mountains. Ecology and Evolution 9:11707–11715.

Harmsen, B. J., R. J. Foster, S. Silver, L. Ostro, and C. P. Doncaster. 2010. Differential use of trails by forest mammals and the implications for camera-trap studies: a case study from Belize. Biotropica 42:126–133.

Hofmeester, T. R., J. P. G. M. Cromsigt, J. Odden, H. Andrén, J. Kindberg, and J. D. C. Linnell. 2019. Framing pictures: a conceptual framework to identify and correct for biases in detection probability of camera traps enabling multi-species comparison. Ecology and Evolution 9:2320–2336.

Hofmeester, T. R., J. M. Rowcliffe, and P. A. Jansen. 2017. A simple method for estimating the effective detection distance of camera traps. Remote Sensing in Ecology and Conservation 3:81–89.

Jackson, R. M., J. D. Roe, R. Wangchuk, and D. O. Hunter. 2006. Estimating snow leopard population abundance using photography and capture-recapture techniques. Wildlife Society Bulletin 34:772–781.

Johnson, D. H. 1980. The comparison of usage and availability measurements for evaluating resource preference. Ecology 61:65–71.

Karanth, U. K., and J. D. Nichols. 1998. Estimation of tiger densities in india using photographic captures and recaptures. Ecology 79:2852–2862.

Kays, R., et al. 2020. An empirical evaluation of camera trap study design: how many, how long, and when? Methods in Ecology and Evolution 11:700–713.

Kellner, K. 2019. jagsUI: A Wrapper Around 'rjags' to Streamline 'JAGS' Analyses. R package version 1.5.1. https://CRAN.R-project.org/package=jagsUI.

Kéry, M., and J. A. Royle 2016. Applied Hierarchical Modeling in Ecology: analysis of distribution, abundance and species richness in R and BUGS. First edition. Academic Press, London, UK.

Kolowski, J. M., and T. D. Forrester. 2017. Camera trap placement and the potential for bias due to trails and other features. PLOS ONE 12:e0186679.

Kolowski, J. M., J. Oley, and W. J. McShea. 2021. High-density camera trap grid reveals lack of

consistency in detection and capture rates across space and time. Ecosphere 12:e03350.

Kuo, L., and B. Mallick. 1998. Variable selection for regression models. Sankhyā: the Indian Journal of Statistics, Series B (1960–2002) 60:65–81.

Linden, D. W., A. K. Fuller, J. A. Royle, and M. P. Hare. 2017. Examining the occupancy–density relationship for a low-density carnivore. Journal of Applied Ecology 54:2043–2052.

Linnell, J. D. C., J. E. Swenson, and R. Andersen. 2000. Conservation of biodiversity in Scandinavian boreal forests: large carnivores as flagships, umbrellas, indicators, or keystones? Biodiversity & Conservation 9:857–868.

Loosen, A. E., O. Devineau, B. Zimmermann, J. P. G. M. Cromsigt, S. E. Pfeffer, C. Skarpe, and K. M. Mathisen. 2021. Roads, forestry, and wolves interact to drive moose browsing behavior in Scandinavia. Ecosphere 12:e03358.

Lukyanenko, R., J. Parsons, and Y. F. Wiersma. 2016. Emerging problems of data quality in citizen science. Conservation Biology 30:447–449.

MacKenzie, D. I., J. D. Nichols, G. B. Lachman, S. Droege, J. A. Royle, and C. A. Langtimm. 2002. Estimating site occupancy rates when detection probabilities are less than one. Ecology 83:2248–2255.

MacKenzie, D. I., J. D. Nichols, J. A. Royle, K. H. Pollock, L. L. Bailey, and J. E. Hines 2006. Occupancy estimation and modeling - inferring patterns and dynamics of species occurrence. Springer, New York, New York, USA.

Mackenzie, D. I., and J. A. Royle. 2005. Designing occupancy studies: general advice and allocating survey effort. Journal of Applied Ecology 42:1105–1114.

Makowski, D., M. S. Ben-Shachar, and D. Lüdecke. 2019. bayestestR: describing effects and their uncertainty, existence and significance within the Bayesian framework. Journal of Open Source Software 4:1541.

Mattisson, J., H. Sand, P. Wabakken, V. Gervasi, O. Liberg, J. D. C. Linnell, G. R. Rauset, and H. C. Pedersen. 2013. Home range size variation in a recovering wolf population: evaluating the effect of environmental, demographic, and social factors. Oecologia 173:813–825.

Mazzamuto, M. V., M. Lo Valvo, and S. Anile. 2019. The value of by-catch data: how species-specific surveys can serve non-target species. European Journal of Wildlife Research 65:68.

McElreath, R. 2020. Statistical rethinking. A Bayesian course with examples in R and Stan. Second edition. CRC Press, Boca Raton, Florida, USA.

McShea, W. J., T. Forrester, R. Costello, Z. He, and R. Kays. 2016. Volunteer-run cameras as distributed sensors for macrosystem mammal research. Landscape Ecology 31:55–66.

Mordecai, R. S., B. J. Mattsson, C. J. Tzilkowski, and R. J. Cooper. 2011. Addressing challenges when studying mobile or episodic species: hierarchical Bayes estimation of occupancy and use. Journal of Applied Ecology 48:56–66.

Morellet, N., et al. 2013. Seasonality, weather and climate affect home range size in roe deer across a wide latitudinal gradient within Europe. Journal of Animal Ecology 82:1326–1339.

Neilson, E. W., T. Avgar, A. C. Burton, K. Broadley, and S. Boutin. 2018. Animal movement affects interpretation of occupancy models from camera-trap surveys of unmarked animals. Ecosphere 9: e02092.

Odden, J., J. D. C. Linnell, and R. Andersen. 2006. Diet of Eurasian lynx, *Lynx lynx*, in the boreal forest of southeastern Norway: the relative importance of livestock and hares at low roe deer density. European Journal of Wildlife Research 52:237–244.

Pease, B. S., C. K. Nielsen, and E. J. Holzmueller. 2016. Single-camera trap survey designs miss detections: impacts on estimates of occupancy and community metrics. PLOS ONE 11:e0166689.

Plummer, M. 2003. JAGS: a program for analysis of Bayesian graphical models using Gibbs sampling. Pages 1–10 *in* Proceedings of the 3rd international workshop on distributed statistical computing. Volume 124, No. 125.10.

R Core Team. 2020. R: a language and environment for statistical computing. R Foundation for Statistical Computing, Vienna, Austria.

Reilly, M. L., M. W. Tobler, D. L. Sonderegger, and P. Beier. 2017. Spatial and temporal response of wildlife to recreational activities in the San Francisco Bay ecoregion. Biological Conservation 207:117–126.

Ren, S., K. He, R. Girshick, and J. Sun. 2015. Faster R-CNN: towards real-time object detection with region proposal networks. Pages 91–99 *in* C. Cortes, N. D. Lawrence, D. D. Lee, M. Sugiyama, and R. Garnett, editors. Advances in neural information processing systems 28. Curran Associates, Inc., Red Hook, New York, USA.

Rich, L. N., D. A. W. Miller, H. S. Robinson, J. W. McNutt, M. J. Kelly, and M. Hayward. 2016. Using camera trapping and hierarchical occupancy modelling to evaluate the spatial ecology of an African mammal community. Journal of Applied Ecology 53:1225–1235.

Rosvold, J., H. Haanes, R. Andersen, K. H. Røed, and K. Bjørneraas 2012. Artenes historie i Norge - bestandsutvikling, genetikk og forvaltning. Pages 34–59 *in* K. Bjørneraas, editor. Klauvvilt i norsk

natur - historie, biologi og forvaltning. Akademika forlag, Oslo, Norway.

Rovero, F., E. Martin, M. Rosa, J. A. Ahumada, and D. Spitale. 2014. Estimating species richness and modelling habitat preferences of tropical forest mammals from camera trap data. PLOS ONE 9:e103300.

Rowcliffe, J. M., C. Carbone, P. A. Jansen, R. Kays, and B. Kranstauber. 2011. Quantifying the sensitivity of camera traps: an adapted distance sampling approach. Methods in Ecology and Evolution 2:464–476.

Royle, J. A., and J. D. Nichols. 2003. Estimating abundance from repeated presence-absence data or point counts. Ecology 84:777–790.

Schenker, N., and J. F. Gentleman. 2001. On judging the significance of differences by examining the overlap between confidence intervals. The American Statistician 55:182–186.

Skogen, K. 2003. Adapting adaptive management to a cultural understanding of land use conflicts. Society & Natural Resources 16:435–450.

Sollmann, R. 2018. A gentle introduction to camera-trap data analysis. African Journal of Ecology 56:740–749.

Steenweg, R., M. Hebblewhite, J. Whittington, P. Lukacs, and K. McKelvey. 2018. Sampling scales define occupancy and underlying occupancy–abundance relationships in animals. Ecology 99:172–183.

Stevens, D. L. 1997. Variable density grid-based sampling designs for continuous spatial populations. Environmetrics 8:167–195.

Stewart, F. E. C., J. T. Fisher, A. C. Burton, and J. P. Volpe. 2018. Species occurrence data reflect the magnitude of animal movements better than the proximity of animal space use. Ecosphere 9:e02112.

Szegedy, C., S. Ioffe, V. Vanhoucke, and A. Alemi 2016. Inception-v4, Inception-ResNet and the impact of residual connections on learning. Pages 4278–4284 *in* Proceedings of the Thirty-First AAAI Conference on Artificial Intelligence (AAAI-17). San Fransisco, California, USA.

Tobler, M. W., S. E. Carrillo-Percastegui, R. Leite Pitman, R. Mares, and G. Powell. 2008. An evaluation of camera traps for inventorying large- and medium-sized terrestrial rainforest mammals. Animal Conservation 11:169–178.

Wong, S. T., J. L. Belant, R. Sollmann, A. Mohamed, J. Niedballa, J. Mathai, G. M. Street, and A. Wilting. 2019. Influence of body mass, sociality, and movement behavior on improved detection probabilities when using a second camera trap. Global Ecology and Conservation 20:e00791.

Zimmermann, F., C. Breitenmoser-Würsten, A. Molinari-Jobin, and U. Breitenmoser. 2013. Optimizing the size of the area surveyed for monitoring a Eurasian lynx (*Lynx lynx*) population in the Swiss Alps by means of photographic capture–recapture. Integrative Zoology 8:232–243.

Zuur, A. F., E. N. Ieno, and C. S. Elphick. 2010. A protocol for data exploration to avoid common statistical problems. Methods in Ecology and Evolution 1:3–14.

DATA AVAILABILITY

All data and scripts used in this manuscript are available from Zenodo: https://doi.org/10.5281/zenodo.4775348. Camera trap images from the lynx-targeted cameras can be found on https://viltkamera.nina.no.

SUPPORTING INFORMATION

Additional Supporting Information may be found online at: http://onlinelibrary.wiley.com/doi/10.1002/ecs2.3662/full